SURFACE SCIENCE SPECTRA
An International Journal & Database Devoted to Archiving Spectra from Surfaces & Interfaces

XPS analysis of Fe2O3-TiO2-Au nanocomposites prepared by a plasma-assisted route

Michael E. A. Warwick, Giorgio Carraro, Elisa Toniato, Alberto Gasparotto, Chiara Maccato, and Davide Barreca

Citation: Surface Science Spectra **23**, 61 (2016); doi: 10.1116/1.4954387
View online: http://dx.doi.org/10.1116/1.4954387
View Table of Contents: http://scitation.aip.org/content/avs/journal/sss/23/1?ver=pdfcov
Published by the AVS: Science & Technology of Materials, Interfaces, and Processing

Articles you may be interested in

TiO2-Fe2O3 and Co3O4-Fe2O3 nanocomposites analyzed by X-ray Photoelectron Spectroscopy
Surf. Sci. Spectra **22**, 34 (2015); 10.1116/1.4934573

A study of Pt/α-Fe2O3 Nanocomposites by XPS
Surf. Sci. Spectra **22**, 47 (2015); 10.1116/11.20150202

Synthesis and characterization of Fe3O4–TiO2 core-shell nanoparticles
J. Appl. Phys. **116**, 114312 (2014); 10.1063/1.4896070

Photocatalytic and antibacterial properties of Au-TiO2 nanocomposite on monolayer graphene: From experiment to theory
J. Appl. Phys. **114**, 204701 (2013); 10.1063/1.4836875

Tuning of the surface plasmon resonance in TiO2/Au thin films grown by magnetron sputtering: The effect of thermal annealing
J. Appl. Phys. **109**, 074310 (2011); 10.1063/1.3565066

HIDEN ANALYTICAL
Instruments for Advanced Science

Gas Analysis
- dynamic measurement of reaction gas streams
- catalysis and thermal analysis
- molecular beam studies
- dissolved species probes
- fermentation, environmental and ecological studies

Surface Science
- UHV TPD
- SIMS
- end point detection in ion beam etch
- elemental imaging - surface mapping

Plasma Diagnostics
- plasma source characterization etch and deposition process reaction
- kinetic studies
- analysis of neutral and radical species

Vacuum Analysis
- partial pressure measurement and control of process gases
- reactive sputter process control
- vacuum diagnostics
- vacuum coating process monitoring

Contact Hiden Analytical for further details:
W www.HidenAnalytical.com
E info@hiden.co.uk
CLICK TO VIEW our product catalogue

Redistribution subject to AVS license or copyright; see http://scitation.aip.org/termsconditions. Download to IP: 147.162.53.201 On: Fri, 01 Jul 2016 14:37:54

XPS analysis of Fe_2O_3-TiO_2-Au nanocomposites prepared by a plasma-assisted route

Michael E. A. Warwick, Giorgio Carraro,[a] Elisa Toniato, Alberto Gasparotto, and Chiara Maccato
Padova University and INSTM, Department of Chemistry, via Marzolo 1, Padova-35131, Italy

Davide Barreca
CNR-ICMATE and INSTM, Department of Chemistry, via Marzolo 1, Padova-35131, Italy

(Received 8 March 2016; accepted 31 May 2016; published 1 July 2016)

Fe_2O_3 nanodeposits have been grown on fluorine-doped tin oxide (FTO) substrates by plasma enhanced-chemical vapor deposition (PE-CVD). Subsequently, the obtained systems have been functionalized through the sequential introduction of TiO_2 and Au nanoparticles (NPs) by means of radio frequency (RF)-sputtering. The target nanocomposites have been specifically optimized in view of their ultimate functional application in solar-driven H_2 generation. In the present study, our attention is focused on a detailed X-ray photoelectron spectroscopy (XPS) characterization of the surface composition for a representative Fe_2O_3-TiO_2-Au specimen. In particular, this report provides a detailed discussion of the analyzed C 1s, O 1s, Fe 2p, Ti 2p, and Au 4f regions. The obtained results point to the formation of pure Fe_2O_3-TiO_2-Au composites, with gold present only in its metallic state and each of the constituents maintaining its chemical identity. © *2016 American Vacuum Society*. [http://dx.doi.org/10.1116/1.4954387]

Keywords: *PE-CVD; RF-Sputtering; Fe_2O_3; TiO_2; Au; nanocomposites*

Accession #s: 01373, 01374, 01375

Technique: XPS

Host Material: #01373: Fe_2O_3-TiO_2-Au; #01374: Au; #01375: Cu

Instrument: Perkin-Elmer Physical Electronics, Inc. 5600ci

Major Elements in Spectra: C, O, Fe, Ti, Au

Minor Elements in Spectra: none

Published Spectra: 6

Spectra in Electronic Record: 8

Spectral Category: technical

INTRODUCTION

Fe_2O_3 has been widely used in sunlight-assisted H_2 generation, mainly via photoelectrochemical (PEC) water splitting, thanks to its advantageous chemico-physical characteristics, such as ample abundance, good photochemical stability in aqueous media and favorable band gap (2.2 eV), allowing the absorption of visible light (Refs. 1–3). Nevertheless, to date some drawbacks are still limiting the efficient exploitation of Fe_2O_3 for PEC aplications, such as the poor charge transport and fast recombination of photogenerated carriers (Refs. 4–7). A strategic solution to overcome the above limitations is offered by the functionalization of iron oxide with suitable agents. In this context, in spite of its wide band gap (3.3 eV) enabling the harvesting of the sole UV light, TiO_2 is an amenable candidate (Refs. 8 and 9). Indeed, the deposition of TiO_2 overlayers on Fe_2O_3 has recently drawn a great deal of attention as an appealing route to improve charge carrier separation and transport (Refs. 3 and 9–15). In addition, the introduction of metal nanoparticles, such as Au ones, can further promote radiation harvesting thanks to the surface plasmon resonance (SPR) phenomenon (Refs. 8 and 16–20), resulting thus in an additional improvement of the composite functional properties.

In the framework of our ongoing research activities, we have recently developed and implemented a plasma-assisted route to Fe_2O_3-TiO_2-Au nanocomposites. In this strategy, iron(III) oxide systems have been synthesized by PE-CVD on FTO substrates under optimized processing conditions, and subsequently functionalized by sequential RF-sputtering of TiO_2 and Au. In particular, in the present contribution a detailed XPS investigation of a representative Fe_2O_3-TiO_2-Au nanocomposite specimen is reported, providing a detailed insight into the surface chemical states of the main elements by the analysis of the principal core level spectra (C 1s, O 1s, Fe 2p, Ti 2p, Au 4f).

[a]Author to whom correspondence should be addressed.

SPECIMEN DESCRIPTION (ACCESSION #01373)

Host Material: Fe_2O_3-TiO_2-Au

CAS Registry #: unknown

Host Material Characteristics: homogeneous; solid; polycrystalline; semiconductor; composite; thin film

Chemical Name: iron (III) oxide - titanium (IV) oxide - gold

Host Composition: Fe, Ti, Au, O

Form: supported nanocomposite

Structure: X-ray diffraction (XRD) analyses revealed the presence of peaks at 24.1, 35.6, 40.9, 49.5°, corresponding to the (012), (110), (113), and (024) reflections of rhombohedral α-Fe_2O_3 (hematite) (Ref. 21), the most thermodynamically stable iron(III) oxide polymorph. No XRD signals related to titania or gold could be detected, likely due to the relatively low amount and high dispersion of the deposited TiO_2 and Au (Ref. 22). High resolution-transmission electron microscopy (HR-TEM) investigation revealed the occurrence of rod-shaped dentritic Fe_2O_3, conformally covered by a TiO_2 overlayer (thickness <5 nm). The fuctionalization with gold resulted in the dispersion of Au nanoparticles (diameter ~50 nm) uniformly decorating the system outermost region.

History & Significance: Fe_2O_3 was deposited using a two-electrode custom-built PE-CVD apparatus equipped with a RF (frequency = 13.56 MHz) generator (Refs. 23 and 24). Experiments were performed using Ar/O_2 plasmas under previously optimized operating conditions (RF-power = 10 W, total pressure = 1.0 mbar, duration = 1 h). The iron precursor, $Fe(dpm)_3$ (Hdpm = 2,2,6,6- tetramethyl-3,5-heptanedione), synthesized according to a previously

Redistribution subject to AVS license or copyright; see http://scitation.aip.org/termsconditions. Download to IP: 147.162.53.201 On: Fri, 01 Jul 2016 14:37:54

reported procedure (Ref. 25), was vaporized in an external glass vessel maintained at 130° C by means of an oil bath, and transported into the reaction chamber by an electronic grade Ar flow (purity = 5.0; flow rate = 60 sccm). Two additional gas lines were used to introduce Ar (flow rate = 15 sccm) and electronic grade O_2 (flow rate = 20 sccm) directly into the reactor chamber. Growth experiments were carried out at a temperature of 100° C on FTO-coated glass substrates (Aldrich®; lateral dimensions = 2.0 cm × 1.0 cm; FTO thickness = 600 nm), fixed on the grounded electrode by means of metallic clips. Prior to each deposition, FTO substrates were cleaned by means of an established procedure (Ref. 24), aimed at minimizing the presence of surface contamination.

Subsequently, TiO_2 dispersion was carried out by RF-sputtering from Ar plasma in the same reactor used for PE-CVD experiments. A Ti target (Alfa Aesar®; thickness = 0.3 mm; purity = 99.95%) was fixed on the RF-electrode, whereas FTO-supported Fe_2O_3 deposits were mounted on the grounded electrode. After preliminary experiments, depositions were performed under the following conditions: substrate temperature = 60° C; Ar flow rate = 10 sccm; total pressure = 0.3 mbar; RF-power = 20 W; sputtering time = 3 h. Subsequently, Au NPs were sputtered starting from an Au target (BALTEC AG; thickness = 0.1 mm; purity = 99.99%), adopting the following experimental parameters: substrate temperature = 60° C; Ar flow rate = 10 sccm; total pressure = 0.3 mbar; RF-power = 5 W; sputtering time = 20 min.

Finally, the obtained specimen was annealed ex-situ in air using a Carbolite HST 12/200 tubular oven for 1 h at 650° C.

As Received Condition: as-grown

Analyzed Region: same as host material

***Ex Situ* Preparation/Mounting:** Specimen mounted as received with a metallic clip on a grounded sample holder and introduced into the analysis chamber through a fast entry lock system.

***In Situ* Preparation:** none

Pre-Analysis Beam Exposure: The analyzed region was exposed to X-ray irradiation for alignment for a period no longer than 5 min.

Charge Control: No flood gun was used. For further details, see Data Analysis Method, Energy Scale Correction.

Temp. During Analysis: 298 K

Pressure During Analysis: $< 10^{-8}$ Pa

INSTRUMENT DESCRIPTION

Manufacturer and Model: Perkin-Elmer Physical Electronics, Inc. 5600ci

Analyzer Type: spherical sector

Detector: multi-channel detector, part number 619103

Number of Detector Elements: 16

INSTRUMENT PARAMETERS COMMON TO ALL SPECTRA

■ *Spectrometer*

Analyzer Mode: constant pass energy

Throughput ($T = E^N$): N = 0

Excitation Source Window: 1.5 μ Al window

Excitation Source: Al K_α

Source Energy: 1486.6 eV

Source Strength: 200 W

Source Beam Size: >25000 μm × >25000 μm

Signal Mode: multichannel direct

■ *Geometry*

Incident Angle: 9°

Source to Analyzer Angle: 53.8°

Emission Angle: 45°

Specimen Azimuthal Angle: 0°

Acceptance Angle from Analyzer Axis: 0°

Analyzer Angular Acceptance Width: 14° × 14°

■ *Ion Gun*

Manufacturer and Model: PHI 04-303A

Energy: 3000 eV

Current: 0.4 mA/cm^2

Current Measurement Method: Faraday Cup

Sputtering Species: Ar^+

Spot Size (unrastered): 250 μm

Raster Size: 2000 μm × 2000 μm

Incident Angle: 40°

Polar Angle: 45°

Azimuthal Angle: 111°

Comment: differentially pumped ion gun

DATA ANALYSIS METHOD

Energy Scale Correction: The reported BEs were corrected for charging phenomena by assigning a BE of 284.8 eV to the adventitious C 1s photopeak (Ref. 36).

Recommended Energy Scale Shift: −0.5 eV

Peak Shape and Background Method: After having performed a Shirley-type background subtraction (Ref. 37), peak position and widths were obtained by means of a least-square fitting procedure, using Gaussian/Lorentzian functions.

Quantitation Method: Atomic concentrations were determined using sensitivity factors from standard PHI V5.4A software (Ref. 38). The peak areas were measured above an integrated background.

ACKNOWLEDGMENTS

The authors acknowledge the financial support under the FP7 project "SOLAROGENIX" (NMP4-SL-2012-310333), as well as from Padova University ex-60% 2012-2015 projects, Padova University SOLLEONE (CPDR132937/13) and ACTION grants, and Regione Lombardia-INSTM ATLANTE project.

Redistribution subject to AVS license or copyright; see http://scitation.aip.org/termsconditions. Download to IP: 147.162.53.201 On: Fri, 01 Jul 2016 14:37:54

REFERENCES

1. A. Duret and M. Grätzel, J. Phys. Chem. B **109**, 17184 (2005).
2. M. Rioult, H. Magnan, D. Stanescu, and A. Barbier, J. Phys. Chem. C **118**, 3007 (2014).
3. D. Barreca *et al*., Adv. Mater. Interfaces **2**, 1500313 (2015).
4. B. Iandolo, B. Wickman, I. Zorić, and A. Hellman, J. Mater. Chem. A **3**, 16896 (2015).
5. J. Y. Kim, G. Magesh, D. H. Youn, J.-W. Jang, J. Kubota, K. Domen, and J. S. Lee, Sci. Rep. **3**, 2681 (2013).
6. F. Le Formal, N. Tetreault, M. Cornuz, T. Moehl, M. Grätzel, and K. Sivula, Chem. Sci. **2**, 737 (2011).
7. J. Lian, X. Duan, J. Ma, P. Peng, T. Kim, and W. Zheng, ACS Nano **3**, 3749 (2009).
8. Z. Zhang, L. Zhang, M. N. Hedhili, H. Zhang, and P. Wang, Nano Lett. **13**, 14 (2013).
9. W.-H. Hung, T.-M. Chien, and C.-M. Tseng, J. Phys. Chem. C **118**, 12676 (2014).
10. A. Banisharif, A. A. Khodadadi, Y. Mortazavi, A. Anaraki Firooz, J. Beheshtian, S. Agah, and S. Menbari, Appl. Catal. B **165**, 209 (2015).
11. Z. Fu, T. Jiang, Z. Liu, D. Wang, L. Wang, and T. Xie, Electrochim. Acta **129**, 358 (2014).
12. J. Krysa, M. Zlamal, S. Kment, M. Brunclikova, and Z. Hubicka, Molecules **20**, 1046 (2015).
13. S. Li, P. Zhang, X. Song, and L. Gao, Int. J. Hydrogen Energy **39**, 14596 (2014).
14. S. J. A. Moniz, S. A. Shevlin, X. An, Z.-X. Guo, and J. Tang, Chem. Eur. J. **20**, 15571 (2014).
15. P. Luan, M. Xie, X. Fu, Y. Qu, X. Sun, and L. Jing, Phys. Chem. Chem. Phys. **17**, 5043 (2015).
16. S. Linic, P. Christopher, and D. B. Ingram, Nat. Mater. **10**, 911 (2011).
17. R. Solarska, K. Bienkowski, S. Zoladek, A. Majcher, T. Stefaniuk, P. J. Kulesza, and J. Augustynski, Angew. Chem. Int. Ed. **53**, 14196 (2014).
18. E. Thimsen, F. Le Formal, M. Grätzel, and S. C. Warren, Nano Lett. **11**, 35 (2011).
19. L. Wang, X. Zhou, N. T. Nguyen, and P. Schmuki, ChemSusChem **8**, 618 (2015).
20. S. C. Warren and E. Thimsen, Energy Environ. Sci. **5**, 5133 (2012).
21. JCPDS, Pattern No. 00-033-0664 (2000).
22. G. Carraro *et al*., RSC Adv. **4**, 32174 (2014).
23. D. Barreca, A. Gasparotto, E. Tondello, C. Sada, S. Polizzi, and A. Benedetti, Chem. Vap. Deposition **9**, 199 (2003).
24. D. Barreca *et al*., Int. J. Hydrogen Energy **38**, 14189 (2013).
25. G. Carraro, C. Maccato, A. Gasparotto, D. Barreca, M. Walter, L. Mayrhofer, M. Moseler, A. Venzo, R. Seraglia, and C. Marega, Phys. Chem. Chem. Phys. **17**, 11174 (2015).
26. J. F. Moulder, W. F. Stickle, P. E. Sobol, and K. D. Bomben, *Handbook of X-ray Photoelectron Spectroscopy* (Perkin Elmer Corporation, Eden Prairie, MN, 1992).
27. G. Carraro, D. Barreca, A. Gasparotto, and C. Maccato, Surf. Sci. Spectra **19**, 1 (2012).
28. D. Barreca, A. Gasparotto, C. Maccato, C. Maragno, and E. Tondello, Surf. Sci. Spectra **14**, 27 (2007).
29. G. Carraro, D. Barreca, E. Comini, A. Gasparotto, C. Maccato, C. Sada, and G. Sberveglieri, CrystEngComm **14**, 6469 (2012).
30. G. Carraro *et al*., RSC Adv. **3**, 23762 (2013).
31. F. Visentin, R. Gerbasi, G. Rossetto, C. De Zorzi, N. El Habra, D. Barreca, and A. Gasparotto, Surf. Sci. Spectra **18**, 29 (2011).
32. X. Zhang, Y. Liu, S. T. Lee, S. H. Yang, and Z. H. Kang, Energy Environ. Sci. **7**, 1409 (2014).
33. Y. Li, H. Yu, C. Zhang, L. Fu, G. Li, Z. Shao, and B. Yi, Int. J. Hydrogen Energy **38**, 13023 (2013).
34. M. Murdoch, G. I. N. Waterhouse, M. A. Nadeem, J. B. Metson, M. A. Keane, R. F. Howe, J. Llorca, and H. Idriss, Nat. Chem. **3**, 489 (2011).
35. D. Barreca, A. Bovo, A. Gasparotto, and E. Tondello, Surf. Sci. Spectra **10**, 21 (2003).
36. D. Briggs and M. P. Seah, *Practical Surface Analysis by Auger and X-ray Photoelectron Spectroscopy*, 2nd ed. (Wiley, New York, 1990).
37. D. Shirley, Phys. Rev. B **5**, 4709 (1972).
38. *Multi-Technique ESCA Operators Reference Manual*, Version 5.2 (Perkin-Elmer, Eden Prairie, MN, 1994), Part No. 625411, Rev. C.

Redistribution subject to AVS license or copyright; see http://scitation.aip.org/termsconditions. Download to IP: 147.162.53.201 On: Fri, 01 Jul 2016 14:37:54

SPECTRAL FEATURES TABLE

Spectrum ID #	Element/ Transition	Peak Energy (eV)	Peak Width FWHM (eV)	Peak Area (eV × cts/s)	Sensitivity Factor	Concentration (at. %)	Peak Assignment
01373-02	C 1s	284.8	2.2	9531	0.296	20.7	Adventitious surface contamination
01373-03[a]	O 1s	530.2	1.7	37391	0.711	33.8	Lattice oxygen in Fe_2O_3 and TiO_2
01373-03[a]	O 1s	531.5	2.7	8483	0.711	7.6	Adsorbed surface -OH and cabonate groups
01373-04	Fe 2p	···	···	125070	2.957	27.2	Fe(III) in Fe_2O_3
01373-04	Fe $2p_{3/2}$	711.3	4.0	···	···	···	···
01373-04	Fe $2p_{1/2}$	724.7	4.6	···	···	···	···
01373-05	Ti 2p	···	···	8953	2.001	2.9	Ti(IV) in TiO_2
01373-05	Ti $2p_{3/2}$	458.5	2.0	···	···	···	···
01373-05	Ti $2p_{1/2}$	464.2	2.7	···	···	···	···
01373-06	Au 4f	···	···	75582	5.240	7.8	Au(0)
01373-06	Au $4f_{7/2}$	84.3	1.6	···	···	···	···
01373-06	Au $4f_{5/2}$	87.9	1.6	···	···	···	···

[a] The sensitivity factor is referred to the whole O 1s signal.

Footnote to Spectrum 01373-02: The C 1s peak can be traced back to the occurrence of adventitious carbon contamination. The slight tailing at higher binding energy can be traced back to the presence of carbonate species arising from atmospheric exposure (Refs. 26 and 27).

Footnote to Spectrum 01373-03: The O 1s region could be fitted by two contributing bands. The dominant one located at BE = 530.2 eV (82% of the total oxygen), is attributed to lattice oxygen in TiO_2 and Fe_2O_3 (Refs. 26–28). The second component, centered at BE = 531.5 eV (18% of the total oxygen), is attributed to surface adsorbed -OH groups and carbonate species due to air exposure (Refs. 26 and 27).

Footnote to Spectrum 01373-04: The Fe 2p spectral shape, along with the positions of the two spin-orbit components [BE (Fe $2p_{3/2}$) = 711.3 eV; Spin Orbit Separation (SOS) = 13.4 eV], were in good agreement with literature values for Fe(III) in Fe_2O_3 (Refs. 26, 27, 29, and 30).

Footnote to Spectrum 01373-05: The main Ti 2p spin-orbit component, Ti $2p_{3/2}$, was centered at BE = 458.5 eV (SOS = 5.7 eV). These values were in line with the presence of Ti(IV) in an oxide environment (Refs. 8, 26, 28, 31, and 32).

Footnote to Spectrum 01373-06: The spectral data for the Au 4f region [BE (Au $4f_{7/2}$) = 84.3 eV; SOS = 3.6 eV] indicated the presence of the sole Au(0) (Refs. 17, 19, 26, and 32–34). The shift in BE value of +0.2 eV compared to that of bulk materials could suggest the occurence of core level shifts (Refs. 34 and 35).

ANALYZER CALIBRATION TABLE

Spectrum ID #	Element/ Transition	Peak Energy (eV)	Peak Width FWHM (eV)	Peak Area (eV × cts/s)	Sensitivity Factor	Concentration (at. %)	Peak Assignment
01374-01[a]	Au $4f_{7/2}$	84.0	1.4	186403	···	···	Au(0)
01375-01[a]	Cu $2p_{3/2}$	932.7	1.6	86973	···	···	Cu(0)

[a] The signal was acquired after Ar^+ erosion.

Redistribution subject to AVS license or copyright; see http://scitation.aip.org/termsconditions. Download to IP: 147.162.53.201 On: Fri, 01 Jul 2016 14:37:54

GUIDE TO FIGURES

Spectrum (Accession) #	Spectral Region	Voltage Shift*	Multiplier	Baseline	Comment #
1373-01	survey	0.5	1	0	1
1373-02	C 1s	0.5	1	0	1
1373-03	O 1s	0.5	1	0	1
1373-04	Fe 2p	0.5	1	0	1
1373-05	Ti 2p	0.5	1	0	1
1373-06	Au 4f	0.5	1	0	1
1374-01 [NP]**	Au $4f_{7/2}$	0.5	1	0	2
1375-01 [NP]	Cu $2p_{3/2}$	0.5	1	0	3

* Voltage shift of the archived (as-measured) spectrum relative to the printed figure. The figure reflects the recommended energy scale correction due to a calibration correction, sample charging, flood gun, or other phenomenon.
** [NP] signifies not published; digital spectra are archived in *SSS* database but not reproduced in the printed journal.
1. Fe_2O_3-TiO_2-Au
2. Au calibration
3. Cu calibration

Redistribution subject to AVS license or copyright; see http://scitation.aip.org/termsconditions. Download to IP: 147.162.53.201 On: Fri, 01 Jul 2016 14:37:54

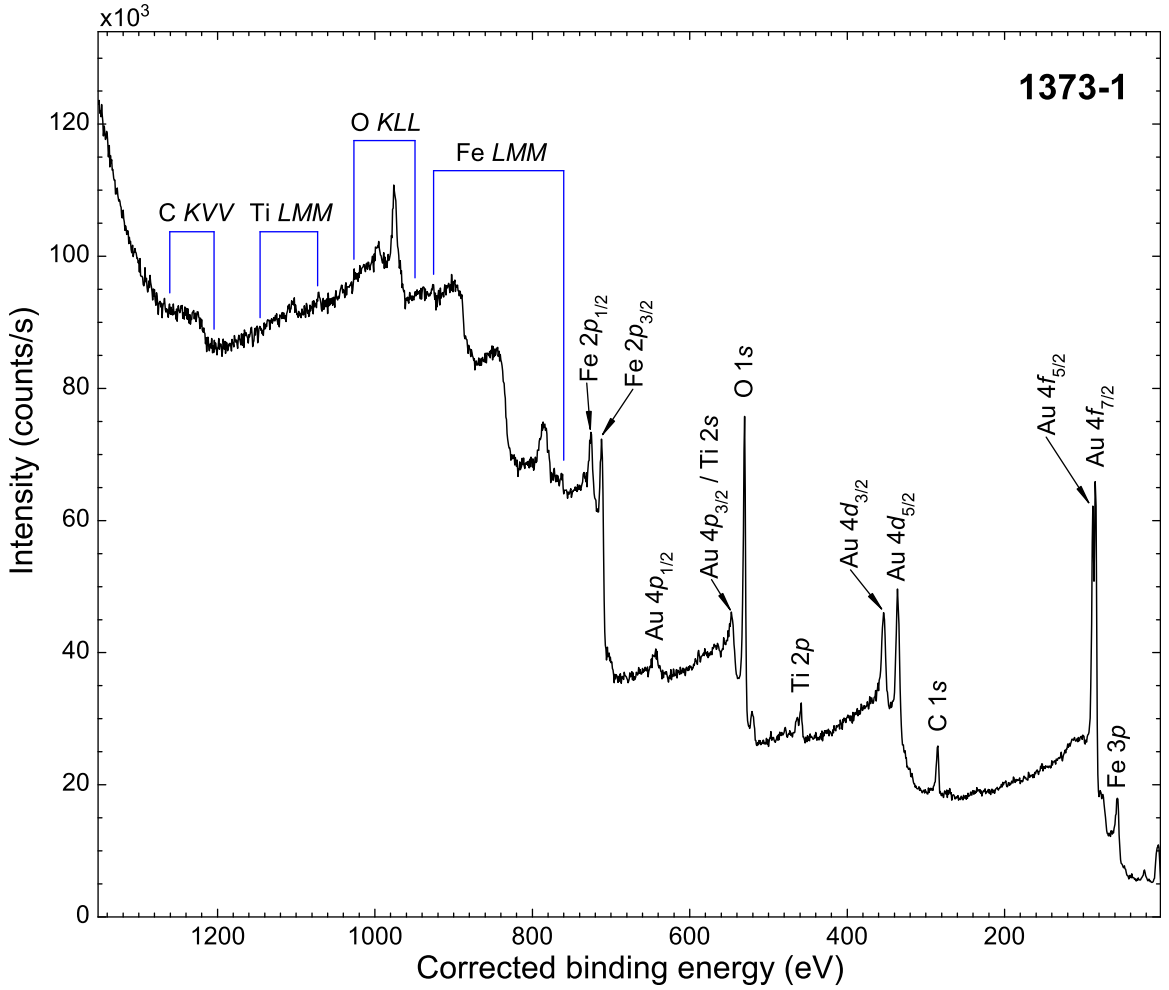

Accession #	01373–01
Host Material	Fe_2O_3-TiO_2-Au
Technique	XPS
Spectral Region	survey
Instrument	Perkin-Elmer Physical Electronics, Inc. 5600ci
Excitation Source	Al K_α
Source Energy	1486.6 eV
Source Strength	200 W
Source Size	>25 mm × >25 mm
Analyzer Type	spherical sector
Incident Angle	9°
Emission Angle	45°
Analyzer Pass Energy:	187.85 eV
Analyzer Resolution	1.9 eV
Total Signal Accumulation Time	303.8 s
Total Elapsed Time	334.2 s
Number of Scans	9
Effective Detector Width	1.9 eV

Redistribution subject to AVS license or copyright; see http://scitation.aip.org/termsconditions. Download to IP: 147.162.53.201 On: Fri, 01 Jul 2016 14:37:54

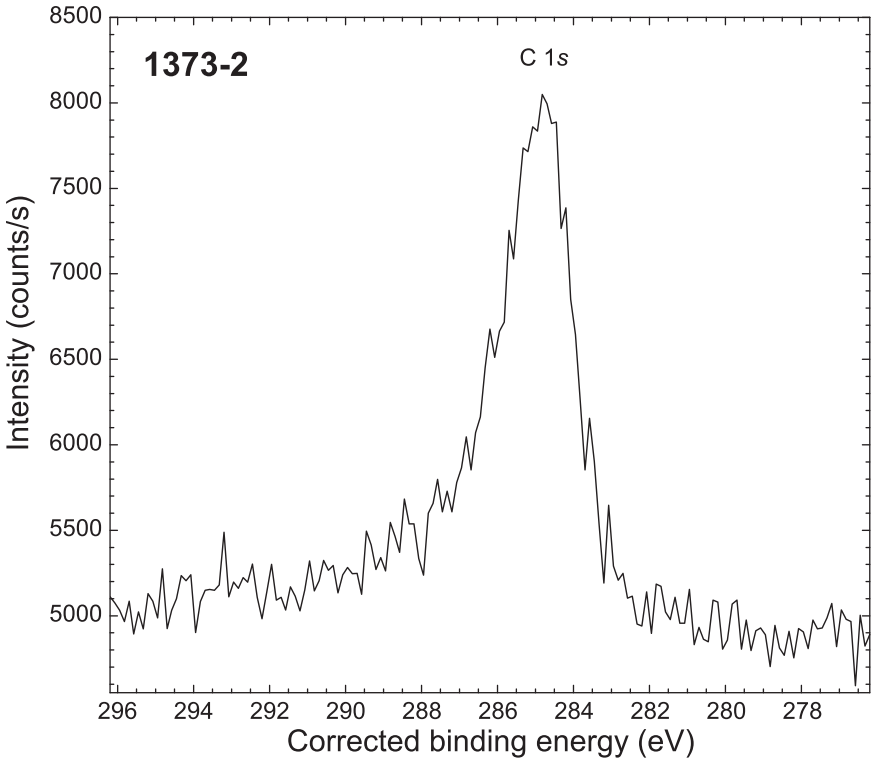

- **Accession #:** 01373–02
- **Host Material:** Fe_2O_3-TiO_2-Au
- **Technique:** XPS
- **Spectral Region:** C 1*s*

Instrument: Perkin-Elmer Physical Electronics, Inc. 5600ci
Excitation Source: Al K_α
Source Energy: 1486.6 eV
Source Strength: 200 W
Source Size: >25 mm × >25 mm
Analyzer Type: spherical sector
Incident Angle: 9°
Emission Angle: 45°
Analyzer Pass Energy: 58.7 eV
Analyzer Resolution: 0.6 eV
Total Signal Accumulation Time: 56.4 s
Total Elapsed Time: 62.0 s
Number of Scans: 7
Effective Detector Width: 0.6 eV
Comment: See footnote below the Spectral Features Table.

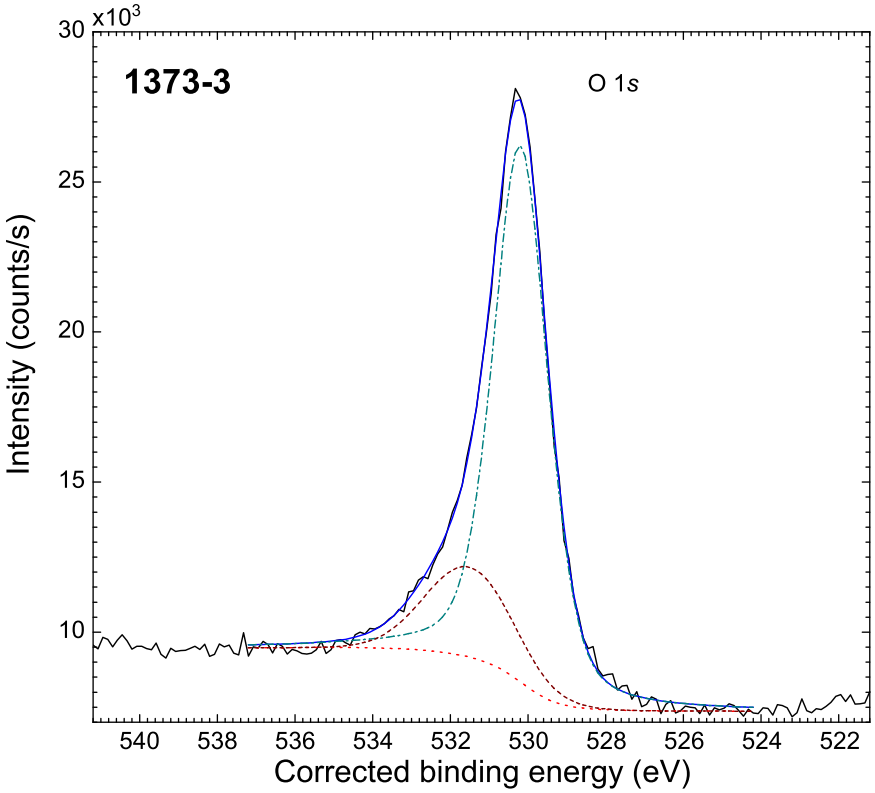

- **Accession #:** 01373–03
- **Host Material:** Fe_2O_3-TiO_2-Au
- **Technique:** XPS
- **Spectral Region:** O 1*s*

Instrument: Perkin-Elmer Physical Electronics, Inc. 5600ci
Excitation Source: Al K_α
Source Energy: 1486.6 eV
Source Strength: 200 W
Source Size: >25 mm × >25 mm
Analyzer Type: spherical sector
Incident Angle: 9°
Emission Angle: 45°
Analyzer Pass Energy: 58.7 eV
Analyzer Resolution: 0.6 eV
Total Signal Accumulation Time: 56.4 s
Total Elapsed Time: 62.0 s
Number of Scans: 7
Effective Detector Width: 0.6 eV
Comment: See footnote below the Spectral Features Table.

Redistribution subject to AVS license or copyright; see http://scitation.aip.org/termsconditions. Download to IP: 147.162.53.201 On: Fri, 01 Jul 2016 14:37:54

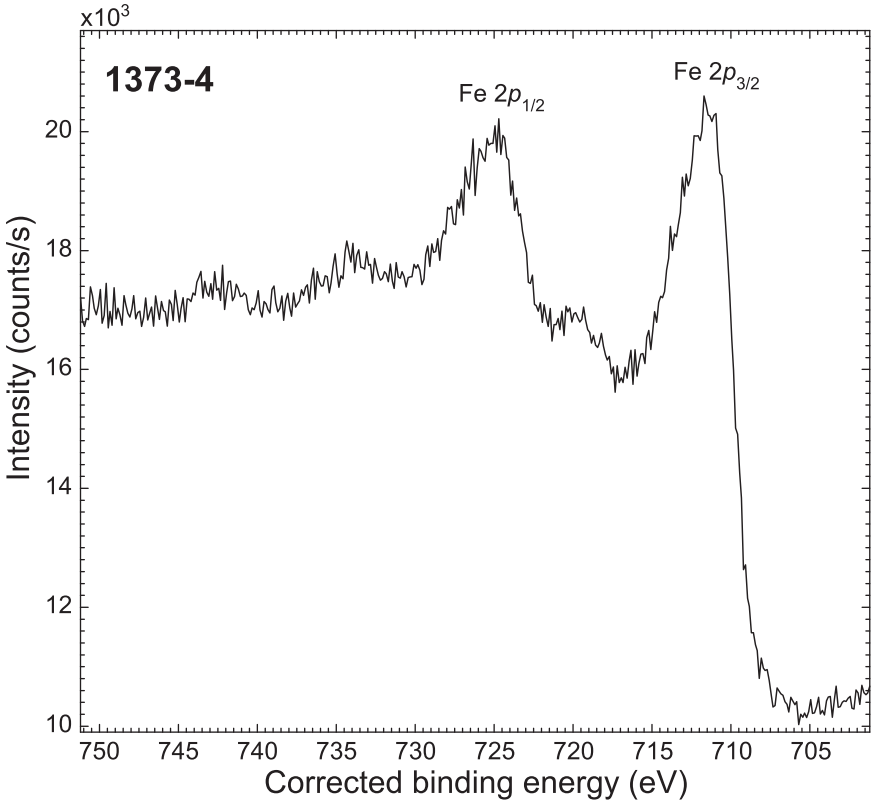

- **Accession #:** 01373–04
- **Host Material:** Fe_2O_3-TiO_2-Au
- **Technique:** XPS
- **Spectral Region:** Fe 2*p*

Instrument: Perkin-Elmer Physical Electronics, Inc. 5600ci
Excitation Source: Al K_α
Source Energy: 1486.6 eV
Source Strength: 200 W
Source Size: >25 mm × >25 mm
Analyzer Type: spherical sector
Incident Angle: 9°
Emission Angle: 45°
Analyzer Pass Energy: 58.7 eV
Analyzer Resolution: 0.6 eV
Total Signal Accumulation Time: 200.5 s
Total Elapsed Time: 220.6 s
Number of Scans: 10
Effective Detector Width: 0.6 eV
Comment: See footnote below the Spectral Features Table.

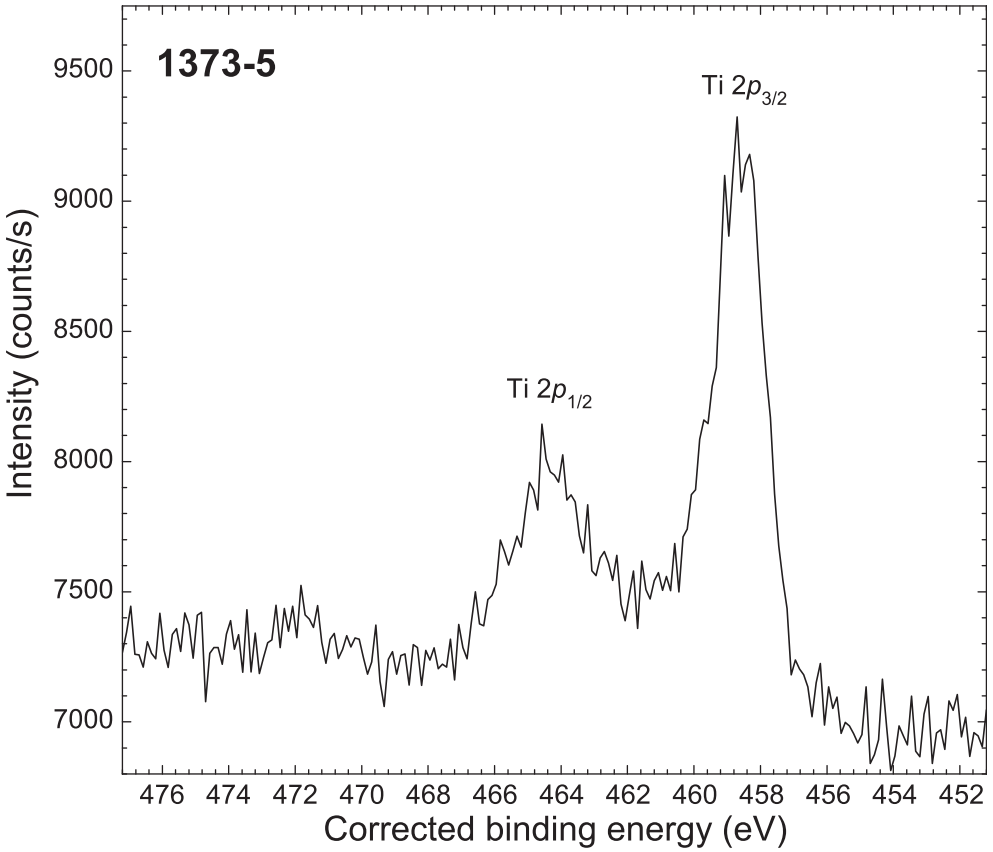

- **Accession #:** 01373–05
- **Host Material:** Fe_2O_3-TiO_2-Au
- **Technique:** XPS
- **Spectral Region:** Ti 2*p*

Instrument: Perkin-Elmer Physical Electronics, Inc. 5600ci
Excitation Source: Al K_α
Source Energy: 1486.6 eV
Source Strength: 200 W
Source Size: >25 mm × >25 mm
Analyzer Type: spherical sector
Incident Angle: 9°
Emission Angle: 45°
Analyzer Pass Energy: 58.7 eV
Analyzer Resolution: 0.6 eV
Total Signal Accumulation Time: 210.0 s
Total Elapsed Time: 231.0 s
Number of Scans: 20
Effective Detector Width: 0.6 eV
Comment: See footnote below the Spectral Features Table.

Redistribution subject to AVS license or copyright; see http://scitation.aip.org/termsconditions. Download to IP: 147.162.53.201 On: Fri, 01 Jul 2016 14:37:54

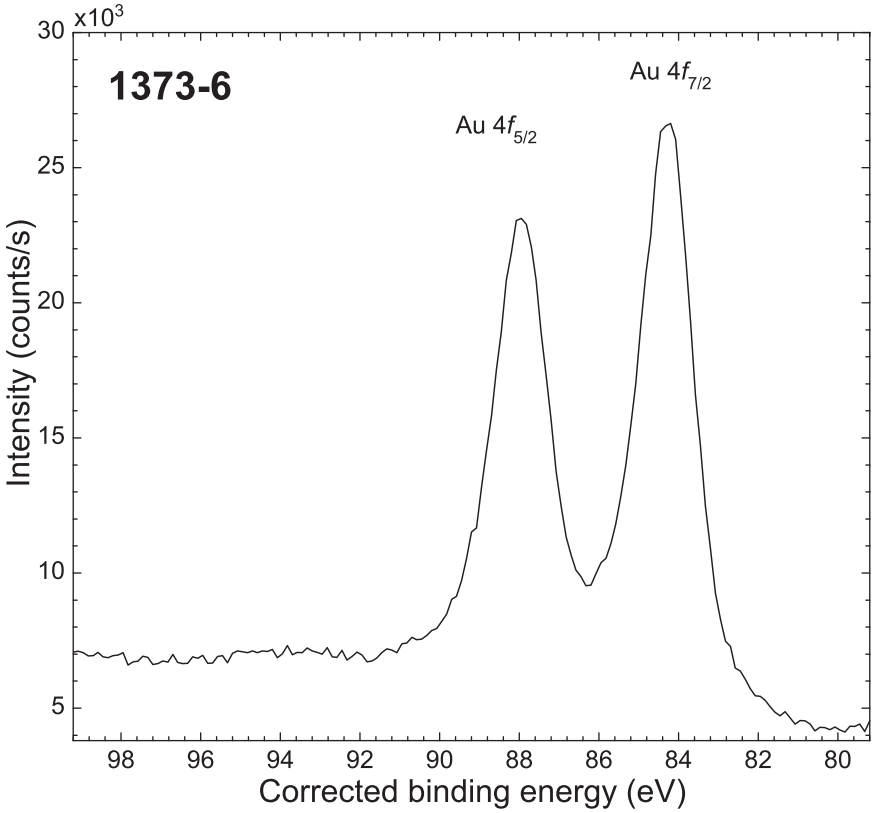

- **Accession #:** 01373–06
- **Host Material:** Fe_2O_3-TiO_2-Au
- **Technique:** XPS
- **Spectral Region:** Au 4*f*

Instrument: Perkin-Elmer Physical Electronics, Inc. 5600ci
Excitation Source: Al K_α
Source Energy: 1486.6 eV
Source Strength: 200 W
Source Size: >25 mm × >25 mm
Analyzer Type: spherical sector
Incident Angle: 9°
Emission Angle: 45°
Analyzer Pass Energy: 58.7 eV
Analyzer Resolution: 0.6 eV
Total Signal Accumulation Time: 80.5 s
Total Elapsed Time: 88.5 s
Number of Scans: 10
Effective Detector Width: 0.6 eV
Comment: See footnote below the Spectral Features Table.

Redistribution subject to AVS license or copyright; see http://scitation.aip.org/termsconditions. Download to IP: 147.162.53.201 On: Fri, 01 Jul 2016 14:37:54